

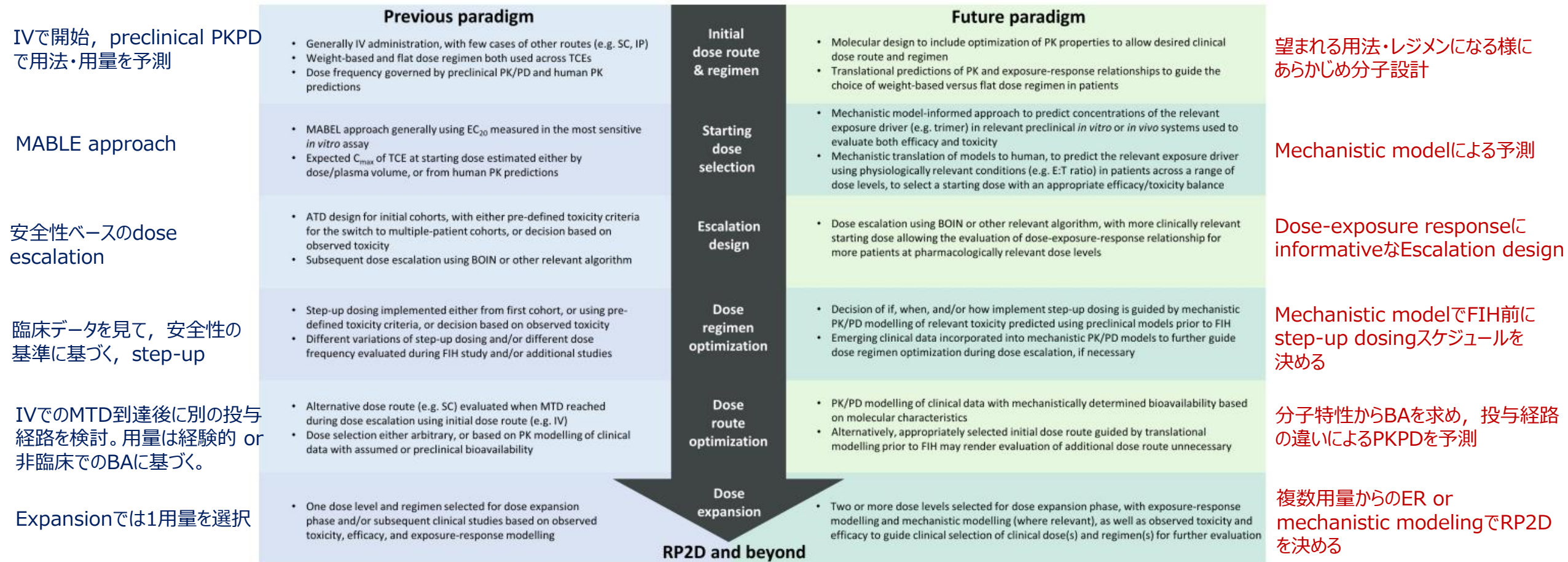
# 最新トピック

演習内容に関連する発展的課題提供

# Contents

- TCE : Mechanistic modeling
  - TCE : CRSの時系列・Grade別のモデリング
  - Tumor growth to PFS/OS
  - Universal Differential Equation
- 
- (おまけ) Vibeコーディング

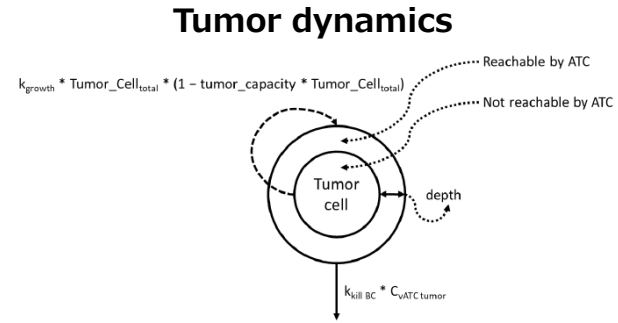
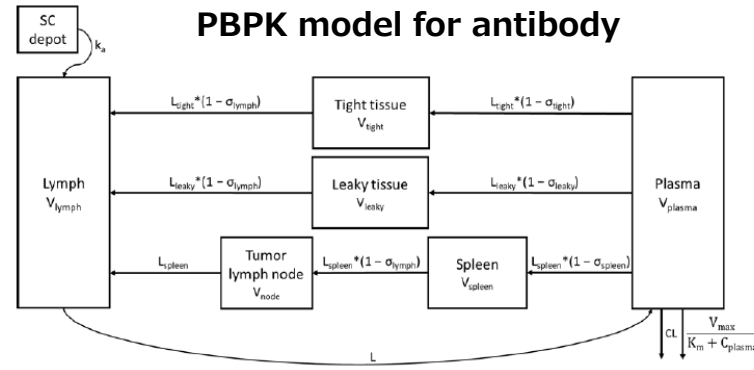
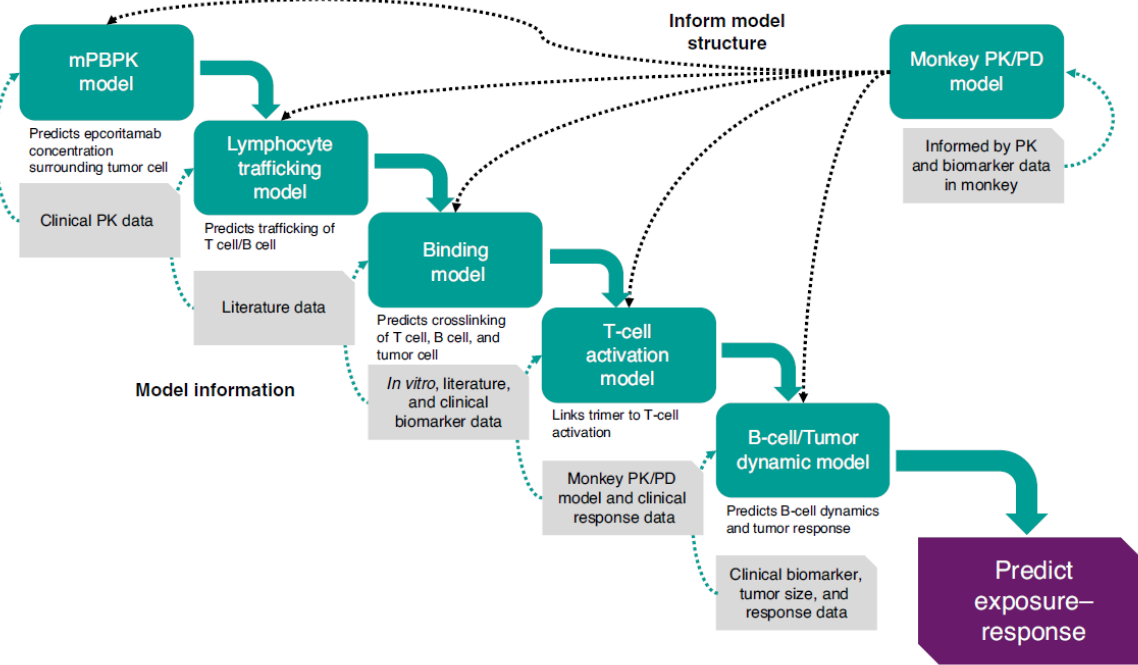
# TCEの臨床用量設定におけるパラダイム



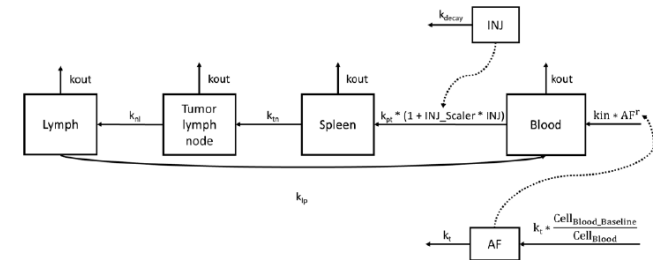
- Preclinical data (in vitro dataを含む) + Modelingで大部分をFIH前に予測
- RP2Dの選択にERを活用できるよう全体を設計

Ball K, Dovedi SJ, Vajjah P, Phipps A. Strategies for clinical dose optimization of T cell-engaging therapies in oncology. *MAbs*. 2023;15(1):2181016. doi:10.1080/19420862.2023.2181016

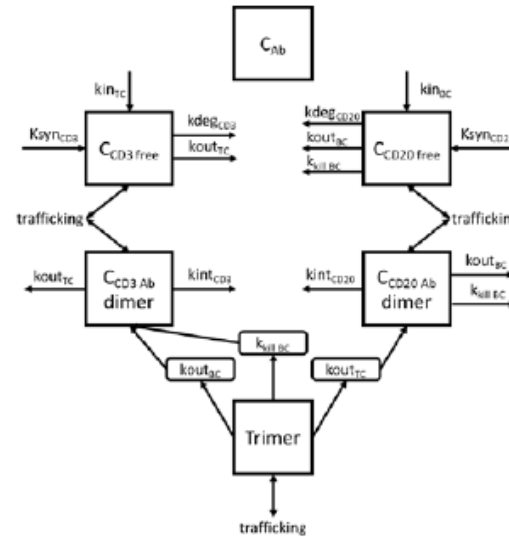
# Semi-Mechanistic PKPD modeling



## Lymphocyte trafficking/turnover



## Antibody-target binding model



## T cell activation

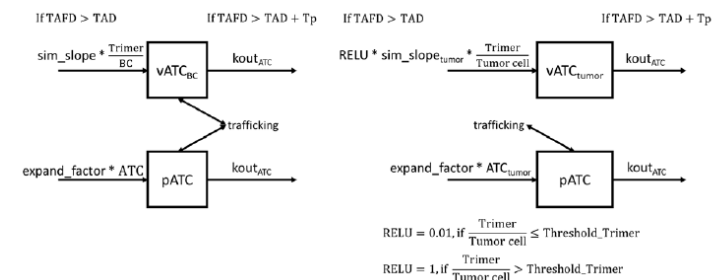


**Figure 1** Semimechanistic PK/PD modeling approach used to inform selection of the recommended phase II dose of epcoritamab. mPBPK, minimal physiologically-based pharmacokinetics; PD, pharmacodynamics; PK, pharmacokinetics.

各メカニズムを記述する半生理学的なモデルを統合して、  
薬剤の曝露-反応性を予測



# Translational QSP modeling

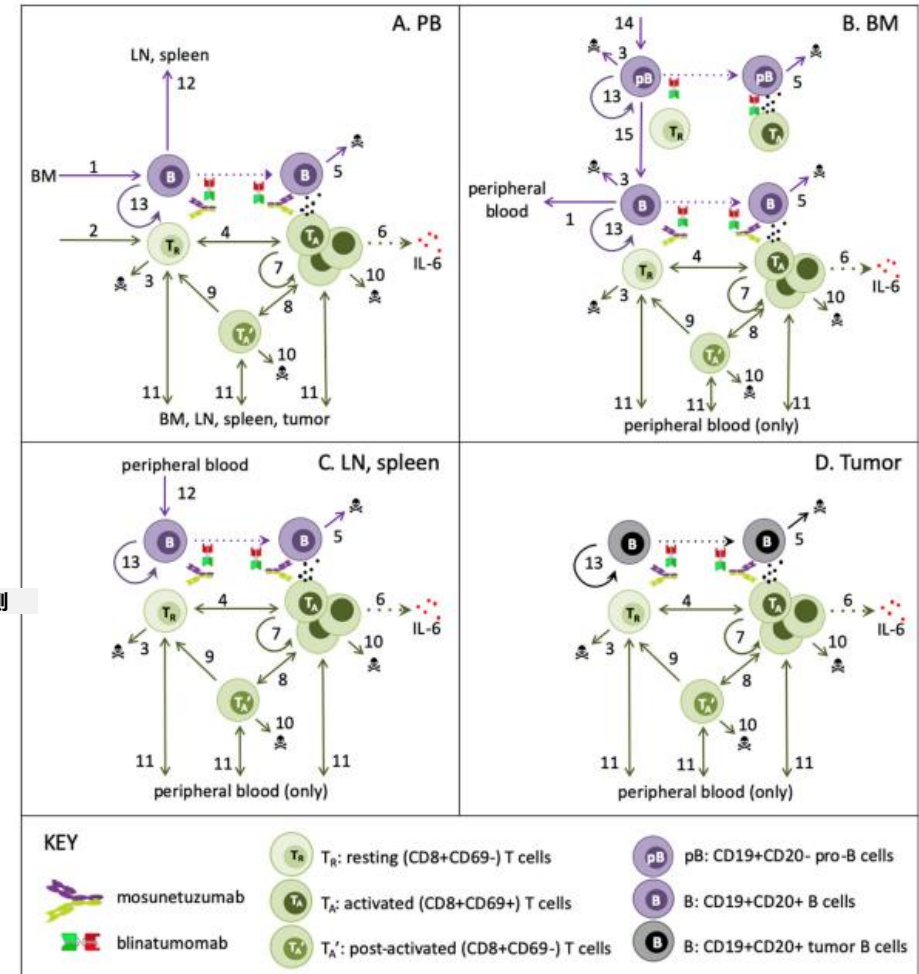
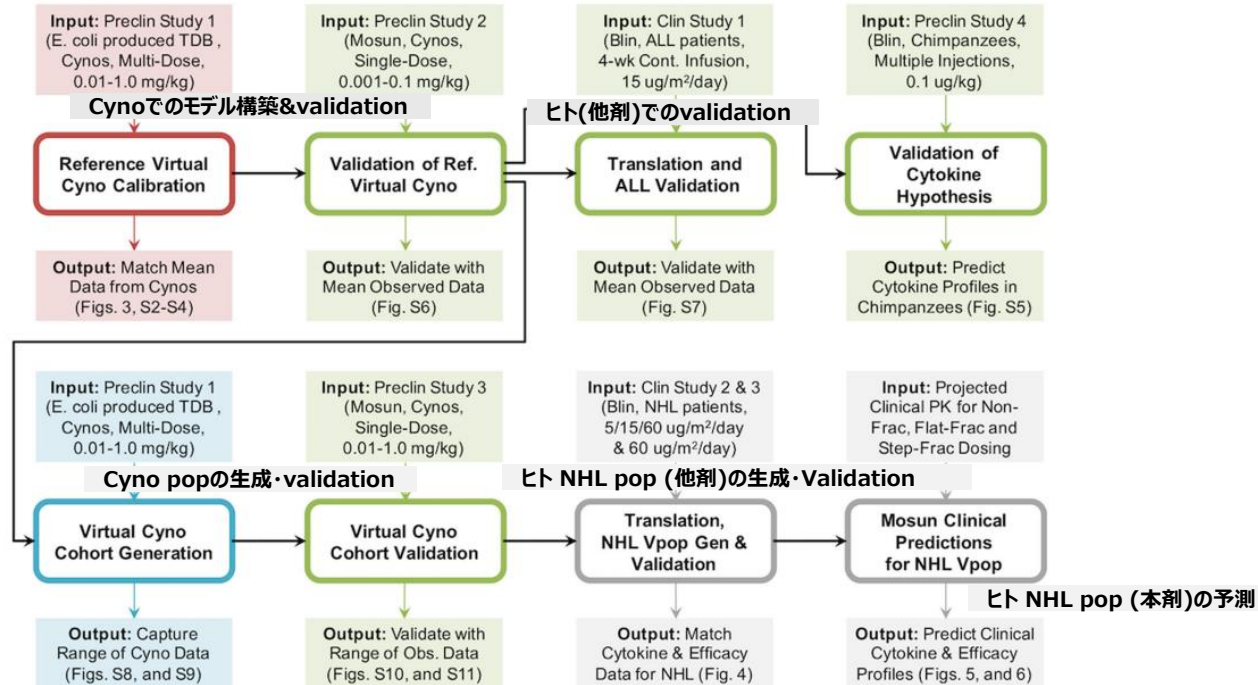


**Fig. 2 Workflow of mosunetuzumab QSP model development.** The QSP model was calibrated using multiple dose preclinical data of E. coli produced anti-CD20/CD3 TDB in cynomolgus monkeys (preclinical study 1, 0.01–1 mg/kg). The outcome was a reference virtual cyno, which reproduces the dynamics of cytokines, B and T-cells in the PB and lymphoid tissues. The model was then validated against data from the single-dose mosunetuzumab in cynomolgus monkeys (preclinical study 2, 0.001–0.1 mg/kg) by using the reference virtual cyno to predict the B and T-cell profiles. Next, the reference virtual cyno was translated to the human ALL patient using the appropriate physiological volume and T and B-cell numbers for different tissues and including blinatumomab PK and its downstream effects on T-cell activation and B-cell killing. The model was successfully validated against the clinical data from blinatumomab in ALL patients. In addition, we used reference virtual cyno and human models to validate the cytokine hypothesis by predicting the IL6 Levels measured in chimpanzees treated with multiple weekly injections of blinatumomab (preclinical study 4). To capture the observed variability in cyno measurements, we generated a virtual cohort of healthy cynos using the range of observed measurements in the multiple dose study of mosunetuzumab in cynomolgus monkeys (preclinical study 1) and validated against the single-dose mosunetuzumab in cynomolgus monkeys (Preclinical study 3, 0.01–1.0 mg/kg). We generated a virtual NHL population by translating the virtual cohort of healthy cynos, adding a tumor compartment by implementing a large B-cell dense mass using human physiology and including additional disease-related variability such as baseline peripheral B and T-cells, tumor load, tumor cell doubling time and revised B:T ratio in the tumor microenvironment. The virtual NHL population matched the distribution of antitumor efficacy and cytokine time profiles following blinatumomab treatment. This population was subsequently used to predict and compare the time course of systemic cytokine levels and antitumor efficacy for different dosing regimens of mosunetuzumab.

血液、リンパ組織、腫瘍組織におけるB細胞・T細胞の動態、サイトカイン産生、腫瘍縮小に対するbi-specific抗体の作用をモデル化



# Translational QSP model → Virtual twins

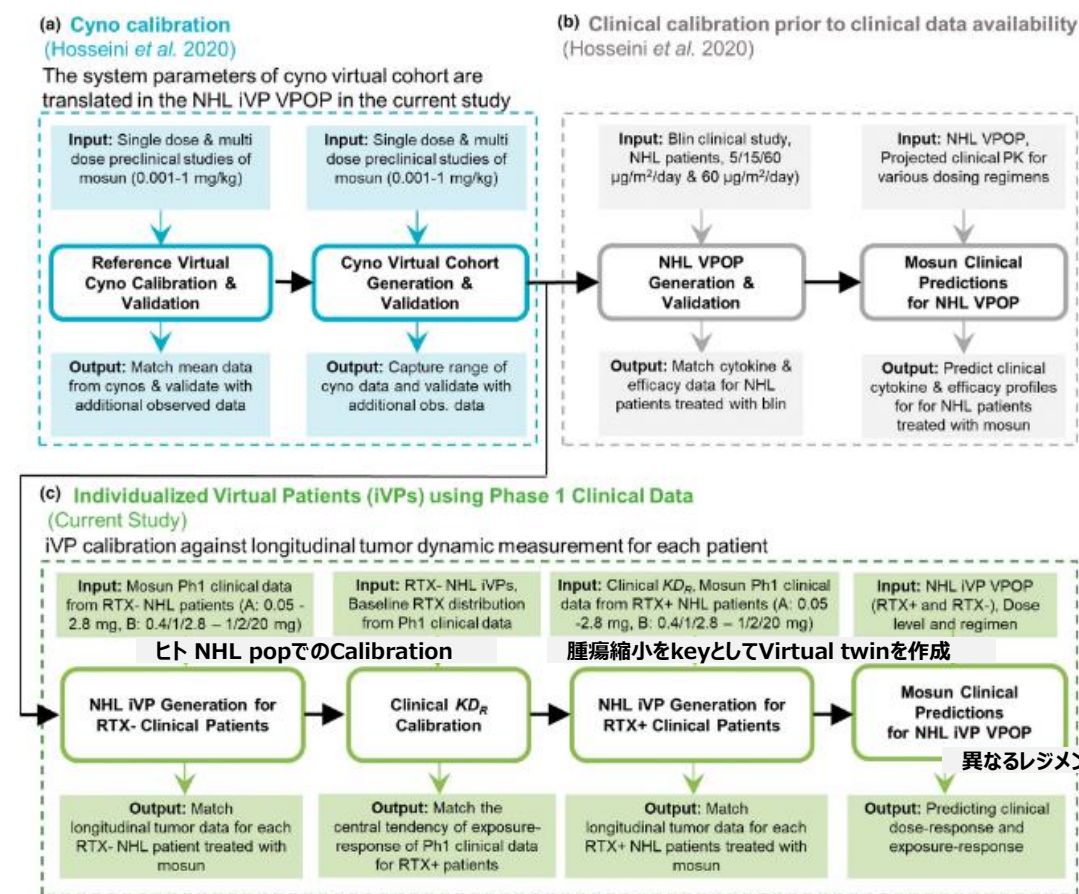
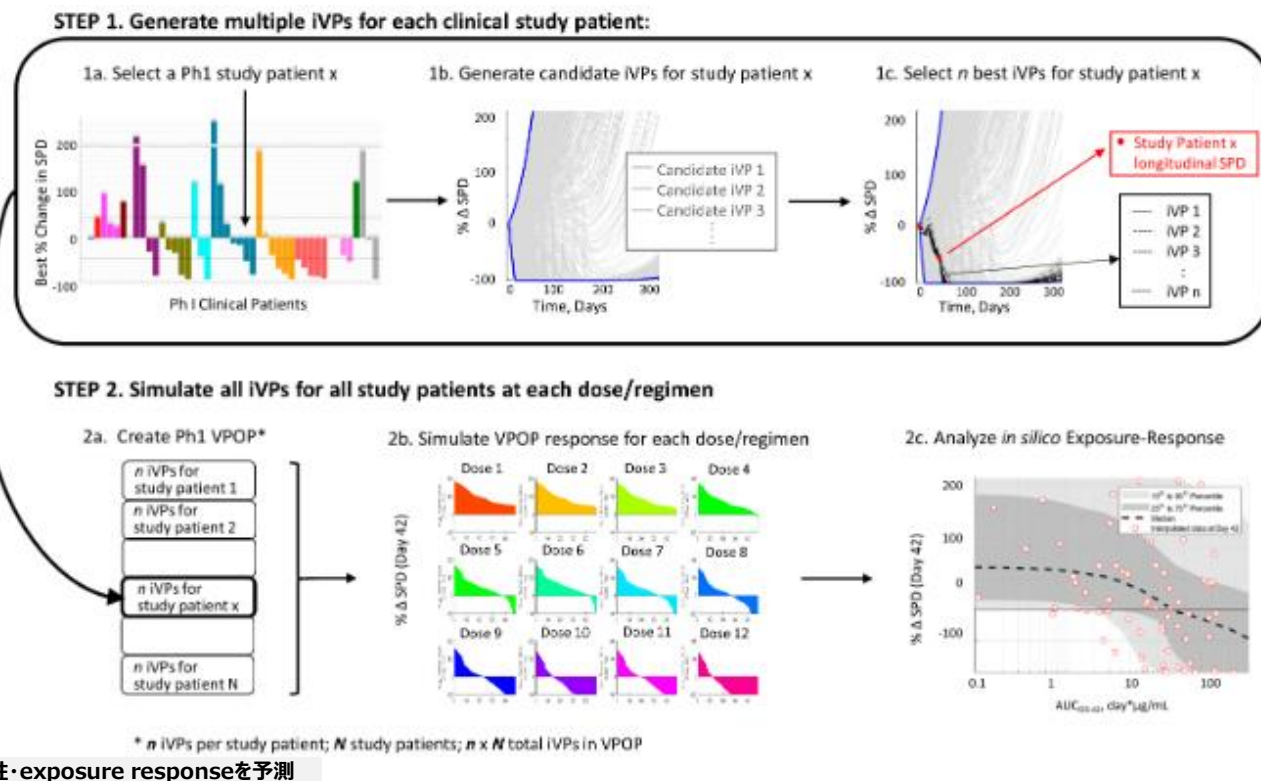


**FIGURE 1** Model development workflow. The (a) cyno calibration and (b) clinical IL-6 calibration based on published blinatumomab data was presented in Hosseini et al.<sup>8</sup> (c) The current study first translates biological variability from the virtual cynos to healthy individuals and then generates a VPOP consisting of iVPs based on mosunetuzumab phase I clinical data. iVP, individualized virtual patient; Mosun, mosunetuzumab; NHL, non-Hodgkin's lymphoma; Ph1, phase I; PK, pharmacokinetic; RTX-, baseline rituximab less than lower level of quantification; RTX+, detectable baseline rituximab; VPOP, virtual population.

Phase I 個別データから生成したVirtual twinで、  
異なる用法・用量での反応性を予測

医薬品開発のためのPPKPDセミナー2025: 上級者コース, 演習2



# TCE + ADC/免疫チェックポイント阻害剤効果予測 併用療法の探索・レジメン設定

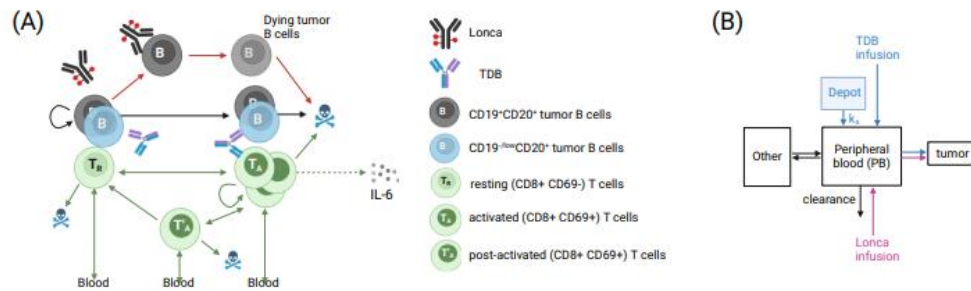


**Fig. 5 | Schematic diagrams for the TDB + loncastuximab tesirine combination therapy model.** **A** compartmental PK diagram. The PK model includes three compartments: a central compartment (i.e., peripheral blood), a peripheral tissue compartment to account for drug distribution, and a deposit compartment to account for subcutaneous injection. **B** Tumor B-cell and T-cell dynamics in the presence of TDB and loncastuximab tesirine. T cells in the tumor cycle through resting state, activated state, and postactivated state (exhausted state), and may die at

any state. Only activated T cells proliferate and induce both healthy and cancerous B-cell death. All T cells could enter or leave the tumor from/the bloodstream. Loncastuximab tesirine could also induce the death of tumor B cells. Tumor cells killed by loncastuximab tesirine transition to a dying stage before being removed from the tumor. Lonca loncastuximab tesirine, PK pharmacokinetic, TDB T-cell-dependent bispecific antibody. Created in BioRender. Li, Y. (2025) <https://BioRender.com/nmbj785>.

Li Y, Wilkins AK, Davis J, et al. QSP modeling of loncastuximab tesirine with T-cell-dependent bispecific antibodies guides dose-regimen strategy. NPJ Syst Biol Appl. 2025;11(1):63. Published 2025 Jun 11. doi:10.1038/s41540-025-00544-8

単剤でのモデルを統合し，併用時の効果を予測  
⇒ 臨床試験デザイン・患者選定の最適化

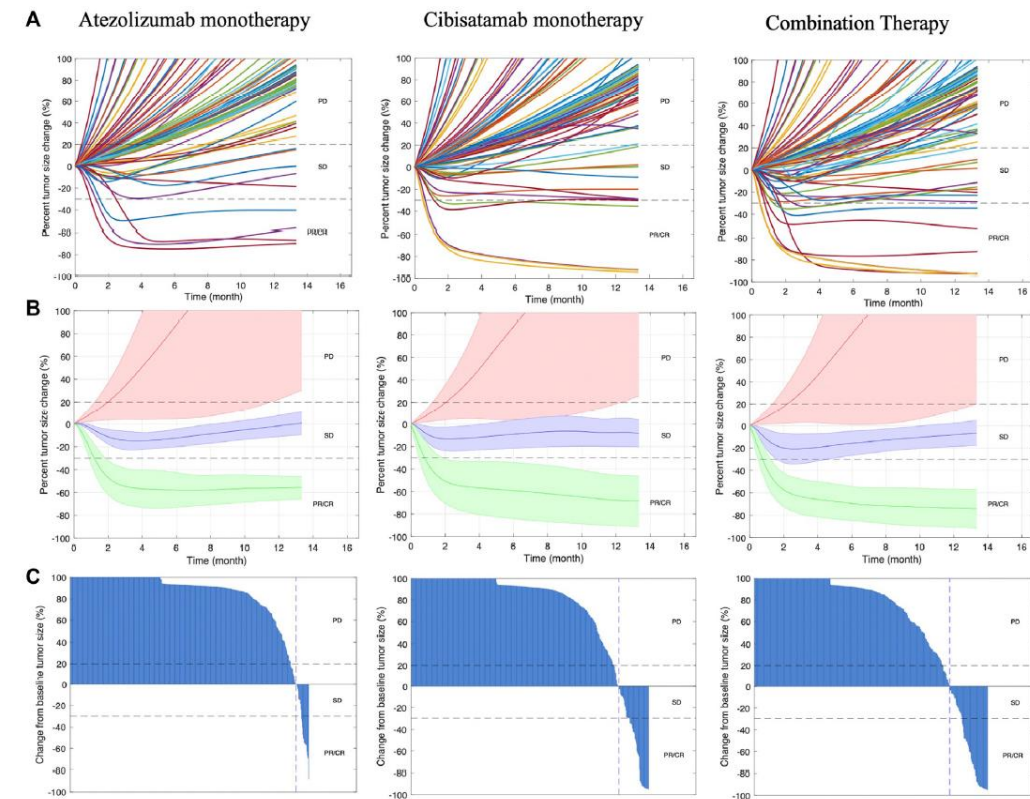


**FIGURE 3**  
Rate of response in model-predicted tumor diameter of (A) 100 randomly selected virtual patients; (B) all VPs. Solid line represents the median and shaded area stands for the median absolute error (mad); (C) best overall response represented by waterfall plots for all VPs. Response is assessed by RECIST 1.1 CR, complete response; PR, partial response; SD, stable disease; PD, progressive disease.

Anbari S, Wang H, Zhang Y, et al. Using quantitative systems pharmacology modeling to optimize combination therapy of anti-PD-L1 checkpoint inhibitor and T cell engager. Front Pharmacol. 2023;14:1163432. Published 2023 Jun 20. doi:10.3389/fphar.2023.1163432



# CRSの時系列・Grade別モデリング

## 隠れ変数-In direct response modelの利用

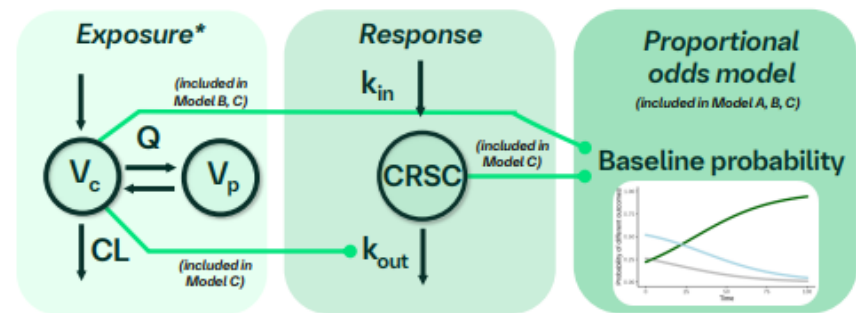


Figure 2.  
Graphical structure  
of the investigated  
PK/PD models.

CL, clearance; CRSC, cytokine release syndrome capacity;  $k_{in}$ , turnover rates; PK/PD, pharmacokinetic/pharmacodynamic;  $V_{c/p}$ , central/peripheral volume of distribution; Q, inter-compartmental clearance.  
\*Individual PK predictions from a preliminary population PK model.

- Model A: 比例オッズモデル
- Model B: 血中濃度を説明変数とした比例オッズモデル
- Model C: 隠れ変数 (CRSC) を説明変数とした比例オッズモデル

CRSの起こりやすさとして隠れ変数を定義し、血中濃度との関係をin-direct response modelを使って記述

Model A  
(AIC: 1165)

Model B  
(AIC: 971)

Model C  
(AIC: 951)

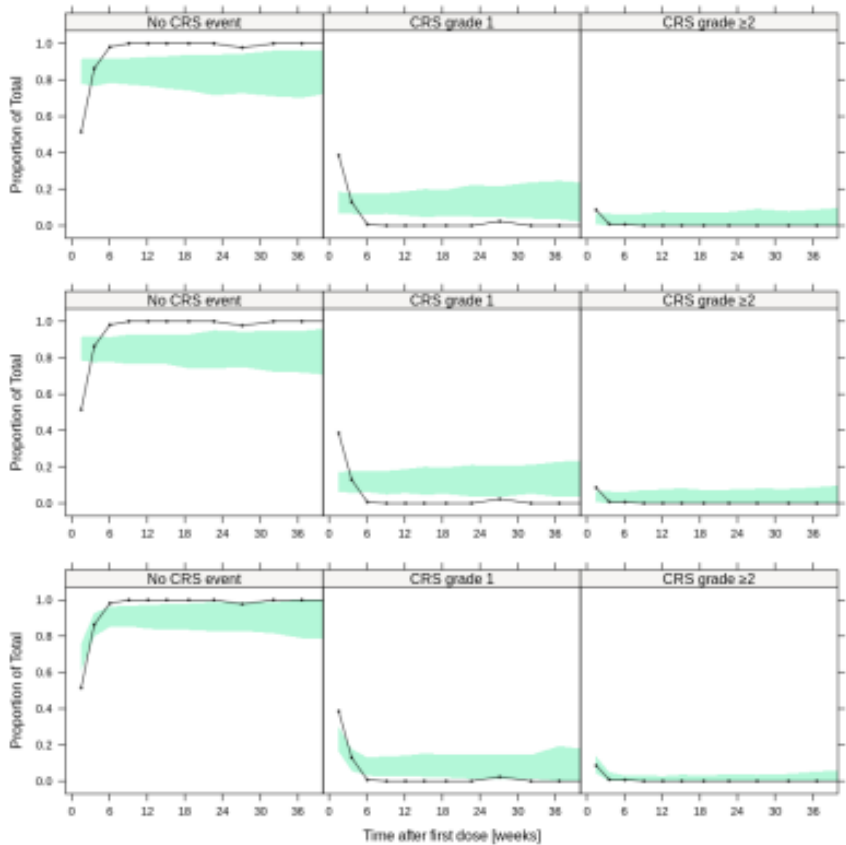


Figure 3.  
Categorical visual predictive checks for weekly target dosing with two step-in doses up to 40 weeks.  
Model A, Proportional odds model; Model B, Proportional odds model with drug effect; Model C, Proportional odds model with drug effect and cytokine release syndrome capacity (CRSC).

500 simulations were performed to create the visual predictive checks. Solid black lines and filled black dots represent the observed proportions of different CRS event grades; shaded green areas represent the 95% confidence intervals; AIC, Akaike information criterion; CRS, cytokine release syndrome.



# CRSの時系列・Grade別モデリング

## Markov modelの利用

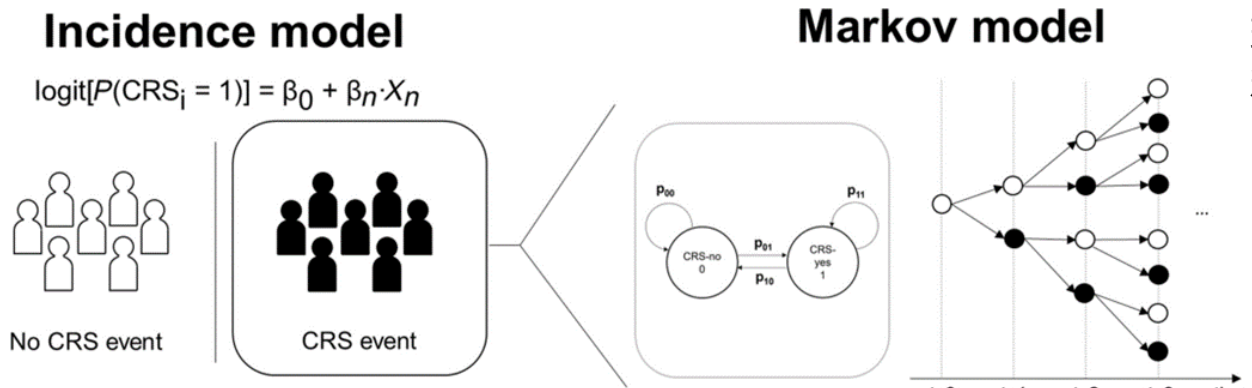


**Figure 1** Two-part mixture model of CRS. The incidence of CRS is described by a logistic regression model where the probability that a patient will have at least one CRS event is dependent upon a baseline probability (or “intercept,”  $\beta_0$ ) as well as covariates, including, but not limited to, drug exposure (or dose). In patients having at least one CRS event, a two-state Markov model (i.e., CRS-yes; 1, or no; 0) describes the evolution of CRS events over discrete-time intervals where the probability to transition between states, or to stay within a state, is estimated from the observed transitions within each patient.

更にSeverity別（Grade別）へ拡張も報告あり

### AN INCIDENCE-SEVERITY MODEL FOR CYTOKINE RELEASE SYNDROME FOLLOWING DOSE-PRIMING REGIMENS OF ELRANATAMAB

Donald Irby<sup>1</sup>, Professor Lena E. Friberg<sup>2</sup>, Professor Mats O. Karlsson<sup>2</sup>, Jennifer Hibma<sup>1</sup>

<sup>1</sup>Pfizer Research and Development, Pfizer Inc, <sup>2</sup>Department of Pharmacy, Uppsala University

PAGE 33 (2025) Abstr 11780 [www.page-meeting.org/?abstract=11780]

### Markov model

現在の状態（CRSあり・なし）→次の時点の状態（CRSあり・なし）の移行確率が現在の状態に依存する

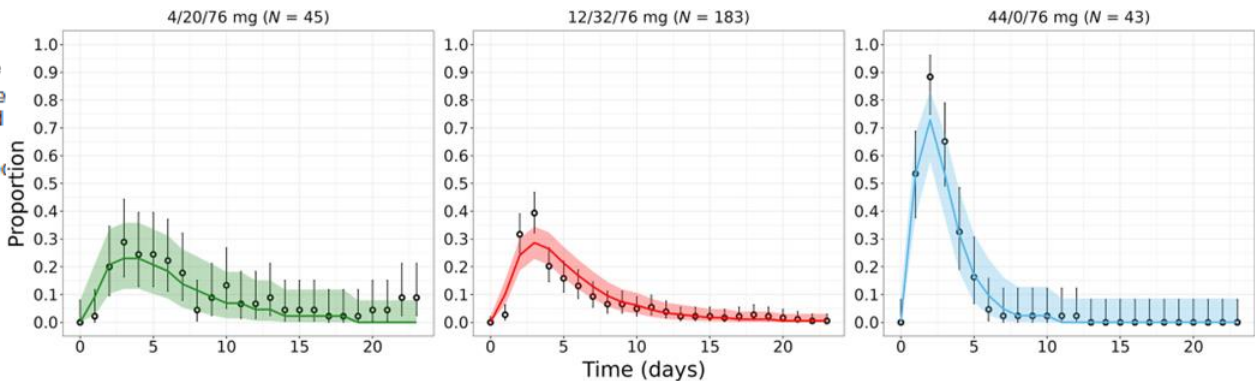


**Figure 3** Population-averaged joint-predicted CRS probabilities over time. Open circles and whiskers represent the observed fraction and 95% CI of grade ≥1 CRS, respectively. The number of patients contributing to the observed summaries per dose-priming regimen are given in the panel titles. Solid lines and shaded regions represent the median and 95% CI of the predictions of grade ≥1 CRS, respectively. The dosing of these amounts occurred on Days 1, 4, and 8.

### 1 Cycle間のCRS発現率を時系列に予測

Irby D, Hibma J, Elmeliegy M, et al. A Novel Two-Part Mixture Model for the Incidence and Time Course of Cytokine Release Syndrome After Elranatamab Dosing in Multiple Myeloma Patients. Clin Pharmacol Ther. 2025;117(6):1687-1695. doi:10.1002/cpt.3533

# Tumor growth inhibition to OS/PFS

## • Joint-modeling

時系列な腫瘍サイズ（経時データ）とイベント型データを統合して解析。異なるデータタイプを同時に扱うことから尤度の計算が煩雑になる。

## • TGI指標からOSを予測

腫瘍サイズの変化を表す指標（TGI metrics）を治療効果の早期予測に使う。  
主なTGI指標：

- TSR（Tumor Size Ratio）：治療開始から一定期間後の腫瘍サイズの変化
- TTG（Time to Tumor Growth）：腫瘍が再び増殖し始めるまでの時間
- TGR（Tumor Growth Rate）：腫瘍の成長速度
- KELIM（CA-125除去速度）：卵巣がんなどで使われる腫瘍マーカーの動態

## • Tumor growth/TGI-OSモデル

- NSCLCでweek 6 TSRからOSを予測

$$\log(T) = \alpha_0 + \alpha_1 \times \text{ECOG} + \alpha_2 \times (\text{Baseline} - 8.5) + \alpha_3 \times \text{PTR}_{\text{wk8}} + \epsilon_{\text{TD}}$$

- TGI + 機械学習モデルでより精度の高いモデルが構築可能

Joint log-likelihood for a patient  $i$ :

$$LL_i(\theta) = \log \int p(y_i | \eta_i; \theta) \{h_i(T_i | \eta_i; \theta)^{\delta_i} S_i(T_i | \eta_i; \theta)\} p(\eta_i; \theta) d\eta_i$$

where

- $\theta$  vector of longitudinal and survival parameters to estimate
- $\eta_i$  vector of random effects
- $p$  density function of the longitudinal process
- No closed-form for the  $LL_i$  if the process is nonlinear
- SAEM algorithm of Monolix extended to joint models<sup>5</sup>

<https://www.fda.gov/media/113417/download>

### TGIとNNの組み合わせ

$$\lambda = \lambda_0 \cdot \kappa \cdot (\lambda_0 \cdot t)^{\kappa-1} / (1 + \lambda_0 \cdot t)^{\kappa}$$

$$\lambda_0 = \lambda_1 \cdot \exp(\beta' \cdot \text{xstd} + \text{NN}_3(\dots))$$

- Log logistic hazard function with neural network  $\text{NN}_3$  to extract features from the covariates and TGD model outputs to inform OS.
- xstd: standardized covariates.
- $\beta$  vector of coefficients in the linear term.
- Inputs to  $\text{NN}_3$ : all baseline covariates (standardized), predicted SLD, PCSLD and rate of change of SLD from the TGD model, all scaled.

<https://acop2024.eventscribe.net/fsPopup.asp?PosterID=690541&mode=posterInfo>

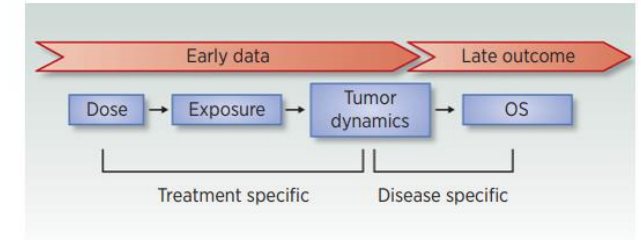
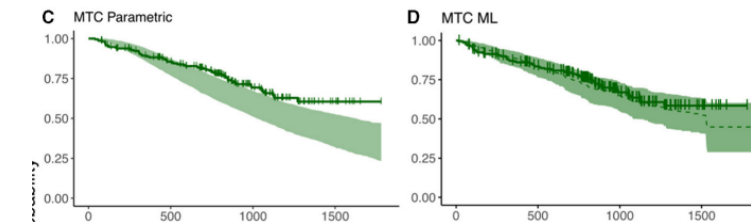


Figure 2.

Tumor growth inhibition as a biomarker to predict OS in oncology (adapted from ref. 50). Early data: tumor dynamic data in phase I, II, interim phase III studies (e.g., at time of PFS readout) but also patient's follow-up at the point of care. Late outcome: OS. Figure reprinted with permission from Bruno and colleagues (Model-based drug development in oncology: what's next?, Clin Pharmacol Ther 2013; copyright John Wiley and Sons).

Clin Cancer Res. 2020 Apr 15;26(8):1787-1795. doi: 10.1158/1078-0432.CCR-19-0287

### 従来モデルとの予測精度の比較



Front Artif Intell. 2024;7:1412865.

# Universal Differential Equation (UDE)

モデルの一部に機械学習モデルを組み込むモデリング手法

従来のMLの様に完全なブラックボックスではなく、数式で記述が難しい部分にのみ機械学習モデルを用いる

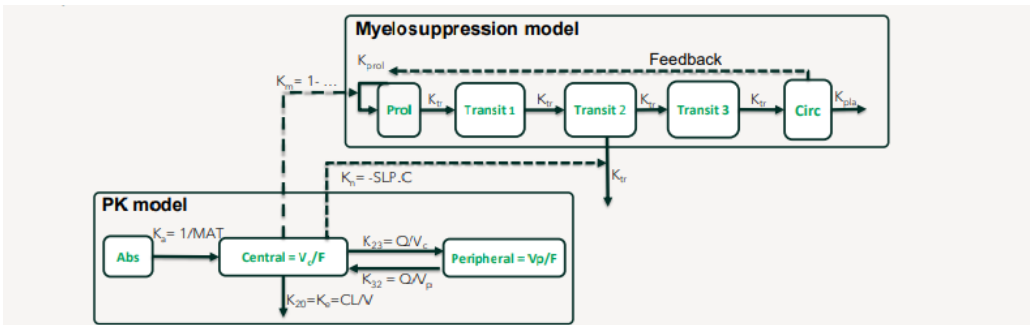


Figure 1. Illustration of the final platelet count model.

Differential equations:

1

$$\frac{d(Abs)}{dt} = -K_a * Abs$$

2

$$\frac{d(Central)}{dt} = K_a * abs - K_{20} * Central - K_{23} * Central + K_{32} * Peripheral$$

3

$$\frac{d(Peripheral)}{dt} = K_{23} * Central - K_{32} * Peripheral$$

4

$$\frac{d(Circ)}{dt} = K_{tr} * Transit3 - K_{sla} * Circ$$

5

$$\frac{d(Prol)}{dt} = K_{prol} * Prol * (1 - EFF) * NN(BL, Circ, T) - K_{prol} * prol$$

6

$$\frac{d(Transit1)}{dt} = K_{tr} * Prol - K_{tr} * Transit1$$

7

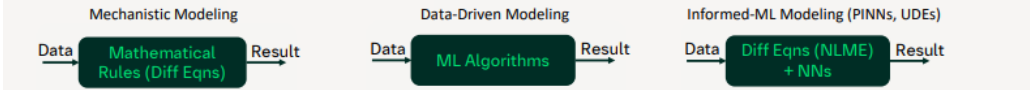
$$\frac{d(Transit2)}{dt} = K_{tr} * Transit1 - K_{tr} * Transit2 - SLP * Central * Transit2$$

8

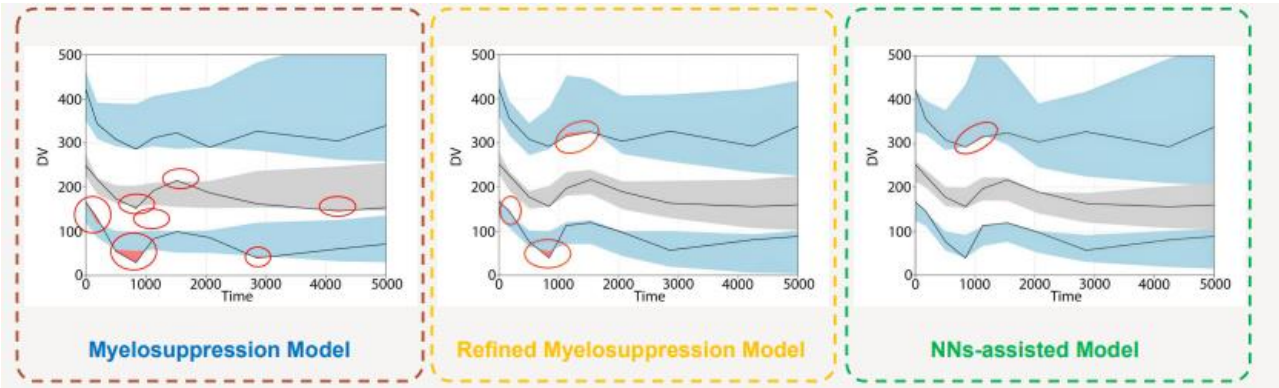
$$\frac{d(Transit3)}{dt} = K_{tr} * Transit2 - K_{tr} * Transit3$$

9 Feedback = (BL/A<sub>0</sub>)

$$\gamma = \theta_1 + \left(1 - \frac{Time^{\theta_2}}{Time^{\theta_2} + \theta_3 \theta_2}\right) \times (Time \times \theta_4)$$



Capabilities	Mechanistic	ML	UDE
Interpretability	✓	✗	✓
Extrapolation	✓	✗	✓
Avoiding overfitting	✗	✗	✗
Modelling complex phenomena	✗	✓	✓
Able to handle small amount of data	✓	✗	✓
Pure data-driven insights	✗	✓	✗



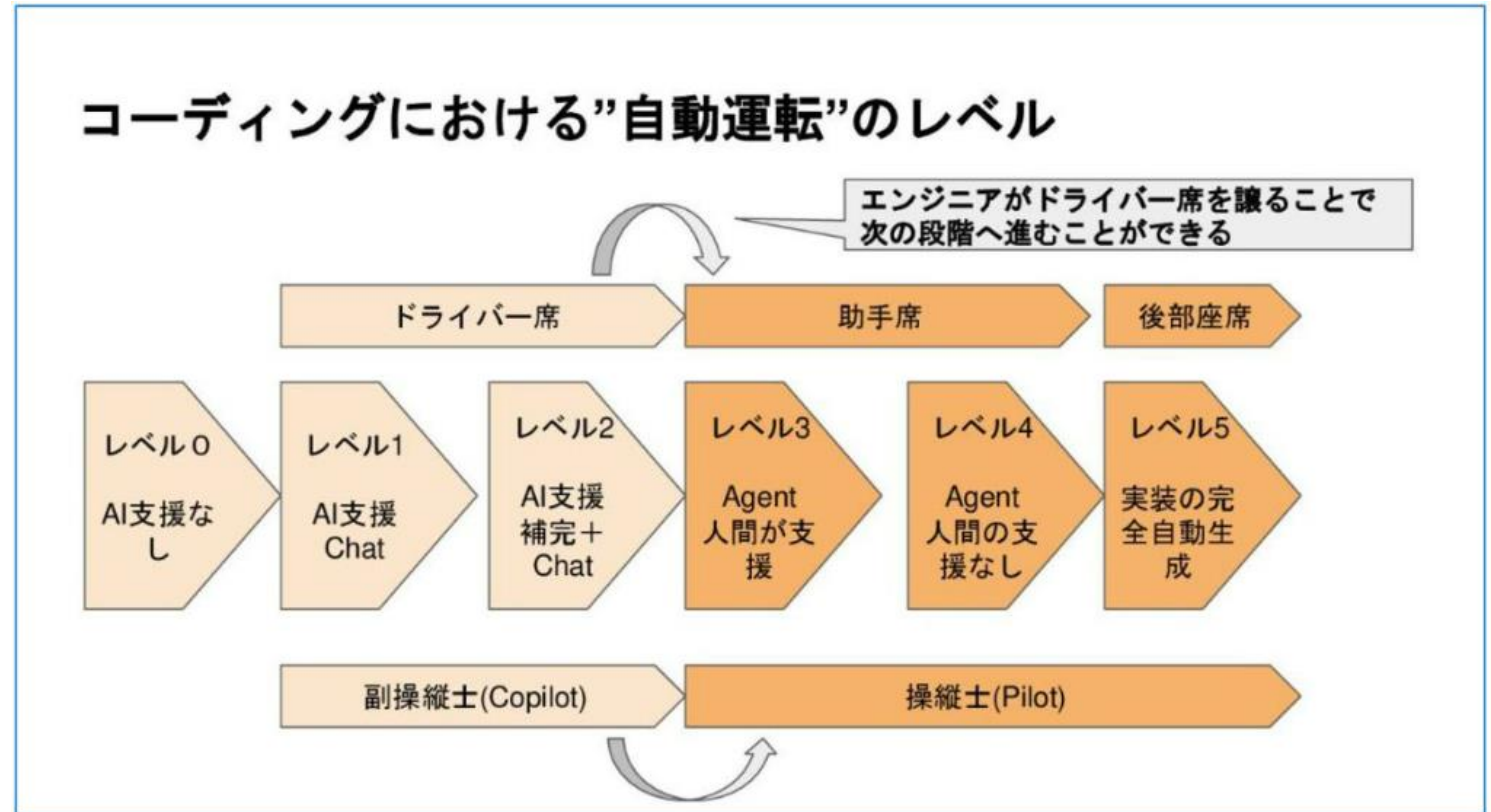
PAGE 32 (2024) Abstr 11106 [www.page-meeting.org/?abstract=11106]



# (おまけ) Vibeコーディング : コーディング技術はいらないかもしれない

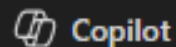
生成AIによるコード生成を行ってくれる開発環境が多数登場。自分でコードを書く必要はない。

- R studio with GitHub copilot
- VS code with GitHub copilot
- Cursor



<https://speakerdeck.com/watany/the-end-of-the-special-time-granted-to-engineers?slide=36>

**テクニックの優位性はなくなり、アイデアの質が大事になる**



ありがとうございます。スライドの内容を踏まえ、未来のファーマコメトリシャンに向けたメッセージを以下にご提案します。

### ✨ 未来のファーマコメトリシャンへのメッセージ

「モデルは進化し、AIは加速する。今、ファーマコメトリクスは“技術”から“戦略”へと進化しています。」

「TCEやADCなど、メカニズムが明確な薬剤では、モデルの力が最大限に発揮される時代です。QSP、Virtual Twin、UDEなど、かつては夢だった手法が現実になっています。」

「コードを書く力よりも、何をモデル化し、どう活用するか。その“問いの質”が、これからのファーマコメトリシャンの価値を決めます。」

「AIが環境を整え、技術の壁を取り払った今こそ、あなたの“構想力”と“洞察力”が輝くときです。」

